Investigation and Testing of Fiber Bragg Grating Sensors for Ultrasonic Applications

Datong Wu, Gabriele Marchi, Janez Rus, Barbara Hopf, Peter Drexler und Johannes Roths
Fakultät für Angewandte Naturwissenschaften und Mechatronik
Hochschule München, 80335 München, E-Mail:datong.wu@hm.edu

Abstract

Broad band frequency response of Fiber Bragg Grating (FBG) sensors in comparison to piezo sensors is interesting for ultrasonic applications e.g. for detection of nonlinearity of ultrasonic waves. In order to increase the sensor sensitivity at higher ultrasonic frequency range (up to 7 MHz) π-phase shifted FBG sensors are manufactured, investigated and tested. The ultrasonic sensor characteristics such as frequency response, directivity were identified. The sensitive π–shifted FBG sensors were then applied for detection of ultrasonic waves in solids (P-, S-, R-waves). The measurement results on a silicone sample show the feasibility of the π–shifted FBG sensors for thickness determination of multiple thin layers. In order to increase the sensor sensitivity at higher frequency the further investigations will be carried out in terms of grating lengths, variations of refraction indexes.

Introduction

In modern nondestructive material testing ultrasound detection becomes one of the most important technology. The conventional piezo transducers are not suitable for harsh environment such as electromagnetic disturbances, high temperature or corrosive areas. Fiber Bragg Grating sensors find already a lot of industrial applications for example as temperature or pressure sensors [1-8]. Many investigations on FBG sensors for ultrasonic applications show the potential of the optical fiber sensors for ultrasonic applications [9-12]. Recent years the π-shifted FBG sensors have been developed for high frequency ultrasound detection due to the higher sensitivity at higher ultrasonic frequency [13-15]. In Fig. 1 the principle of the π-shifted FBG sensors is shown.

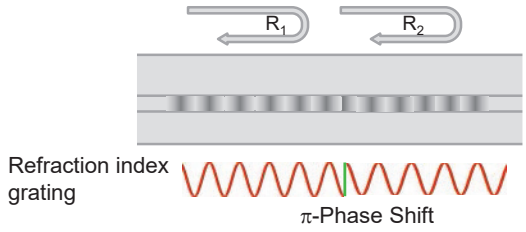

Fig. 1: Schematic diagram of reflections (R_1 and R_2) in a π-shifted FBG sensor. The modulated refractive index shows a 180° phase jump in the middle of the fiber grating. The modulation of the refractive index in the optical fiber core operates like two gratings for the incoming laser beam.

The modulation of the refractive index in the fiber core has a phase jump of 180° in the middle of the grating length and can be considered as two identical Bragg gratings, which have a phase difference of 180°. Part of optical waves in the fiber will be reflected, if the wavelengths of the incident spectrum meet the Bragg condition (1):

$$\lambda_B = 2n_{eff}\Lambda \qquad (1)$$

where λ_B is the Bragg wavelength, Λ is the grating period and n_{eff} is the effective refractive index of the mode in the fiber core. The π-shifted grating main characteristic is the production of a destructive interference between the reflections produced from the grating parts on the left and on the right of the π-shift (Fig. 2) at the Bragg wavelength. The resulting effect is a narrow pass band region (π-shifted dip) in the reflectivity spectrum around λ_B.

Figure 2 shows the operating principle of the π-shifted FBG sensors. A laser beam with a narrow band emission can be tuned to the operating point, halfway of the sideline of the (π-shifted dip, where a rapid change of the intensity with the wavelength exists. Due to ultrasonic waves the fiber grating length and refractive index change slightly, which induce small shift of the reflection spectrum (blue line). In consequence a large change on the laser beam intensity will occur (red line), which can be registered with a photodiode. The variation of the Bragg wavelength is proportional to sound wave pressure changes Δp, where the proportionality depends on the opto-elastic effect of the glass fiber (2).

$$\frac{\Delta\lambda}{\lambda_B} = \frac{\Delta\Lambda}{\Lambda} + \frac{\Delta n}{n_{eff}} = \left(\frac{\partial\Lambda}{\Lambda\partial p} + \frac{\partial n}{n_{eff}\partial p}\right)\Delta p \qquad (2)$$

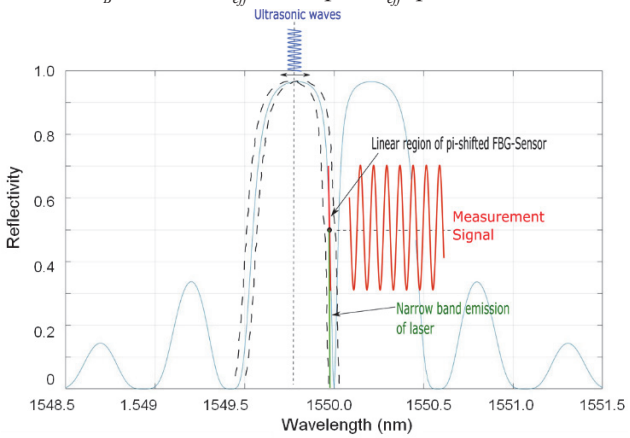

Fig. 2: Principle of the π-shifted FBG sensors. The sensitivity of the π-shifted FBG sensors can be increased with the rapid slope change at the operating point.

A model of the π-shifted grating was also developed using transfer matrix method and an investigation of the effects of ultrasound waves on the spectra was pursued. Based on the investigations on the passive π-shifted FBG sensors a new kind of active π-shifted FBG sensor with much higher sensitivity is in developing for ultrasonic applications.

Experimental procedures

The π-shifted FBG used for the ultrasound detection were produced using the phase-mask technique [16] in a facility of the Munich University of Applied Sciences. The setup is shown in Figure 3 with the reference coordinates. The laser beam used for the inscription of the π-shifted FBG was

produced by a KrF excimer laser (MLI-200 KRF FBG, MLase, Germering, Germany). The laser beam had a wavelength of 248 nm and a cross section of about 3 mm. The beam was directed by two mirrors towards a cylindrical lens to focus the beam in y direction at about 150 mm distance. A π-shifted phase mask (OEland Inc., Lassale, Canada) with a period of 1075.5 nm, 25 mm length along the x direction and 3 mm width along the y direction was placed few mm before the lens focal point to produce an interference pattern of 537.25 nm period.

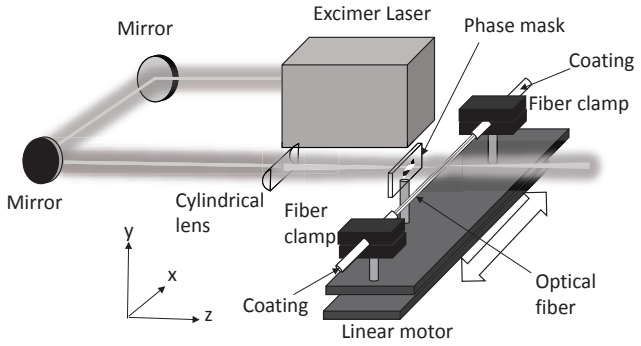

Fig. 3: Setup for the manufacturing of FBG and reference coordinates in the Photonik-Lab of Hochschule München.

A portion of the coating of a photosensitive fiber (GF1B, Nufern, East Granby, US) was removed and the part without coating was placed in front of the phase mask at about 200 µm distance. The fiber was stretched along the length of the mask (x-direction) as in Figure 3 and hold by two fiber clamps. The mask and the fiber clamps were both mounted on a linear DC motor (M-403.8DG, Physik Instrumente, Karlsruhe, Germany) of 316 mm maximum travel, which could shift the mask and the fiber together in the x direction.
For the inscription the laser pulse intensity was set at 5 mJ and at a pulse repetition rate of 100 Hz. The phase mask was initially in a position outside the beam path. Then the motor started to drive the mask and the fiber towards the beam path at a speed of 0.1 mm/s. During the passage of the mask through the beam a 25 mm π-shifted FBG was inscribed. After the mask made a complete passage through the laser path, the laser beam was blocked and the FBG was taken out of the clamps. The spectrum of the FBG was measured with a scanning DFB (Distributed FeedBack) laser (LD-1550-0030-DFB-1, Toptica AG, Dachau, Gemany) and can be seen in Figure 4. It showed a small dip in the middle produced from the π-shift of the grating. The dip in the figure has a FWHM of about 6 pm and a Wavelength of about 1549.7 nm.

The units of voltage and ms are diode signal, control signal and scanning time, respectively. The scanning time is corresponding to the wavelength of the spectrum.
The π-shifted FBG sensors can be modeled with uniform divided grating elements based on the transfer matrix method [17]. Fig. 5 is the simulation results of a π-shifted FBG sensor with the middle wavelength at 1550 nm.

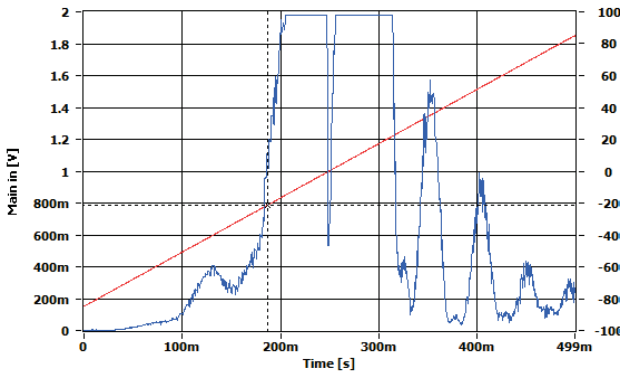

Fig. 4: Spectrum of a π-shifted FBG sensor (blue line) and line scan of the wavelength (red line), Grating parameters: 24 mm grating length, 535 nm grating distance. The plateau at 2 V is due to intensity saturation of the detector

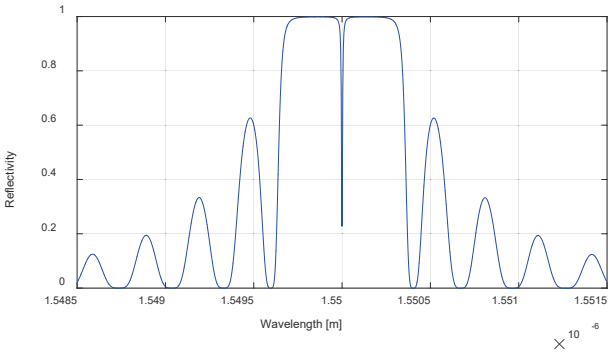

Fig. 5: Simulation result based on the transfer matrix of fiber grating elements show the reflected FBG spectrum.

The DFB laser is used for evaluate spectrum characteristics of π-shifted FBG sensors with the wavelength sweep from 1545 nm to 1555 nm (Fig. 6). For the ultrasonic measurements the laser wavelength is adjusted at the operating point, where the slope is maximum for the highest sensitivity.

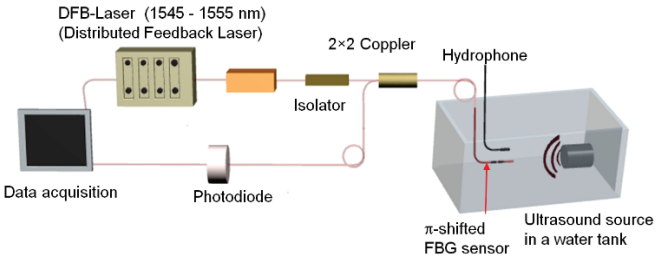

Fig. 6: Measurement setup with a water tank for the sensor characterization. For comparison a hydrophone is used.

Characterization of π-shifted FBG Sensors

The frequency response of π-shifted FBG sensors was investigated using continuous ultrasonic wave generator. The ultrasonic frequency can be changed stepwise from 1 MHz to 10 MHz, whereas the amplitude was not changed during this measurement. For these measurement signals were averaged 500 times. The frequency range from 1 MHz to 10 MHz is the most interesting for industrial and biomedical applications.
The intensity of the hydrophone signal shows quite constant in this frequency range. In comparison the results of the

π-shifted FBG sensor show the signal amplitude becomes smaller at higher frequency (Fig. 7). Signal at frequency higher than 7 MHz becomes much smaller for this measurement configuration. At higher frequency therefore the signal to noise ratio becomes relevant for applications.

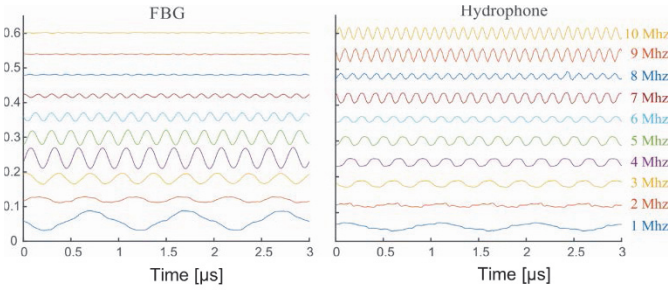

Fig. 7: Frequency responses of the π-shifted FBG sensor (left) and hydrophone (right) using continuous ultrasound waves stepwise from 1 MHz to 10 MHz.

In order to investigate the directivity of the π-shifted FBG sensors, the angle α between the axis of the π-shifted FBG sensor and the direction of the piezo ultrasonic sources at 1 MHz, 2 MHz and 4 MHz was changed.
In the case of α = 90° the signal amplitudes were 4 -10 times higher than at incident angle of α = 0° and α = 45° (Fig. 8).

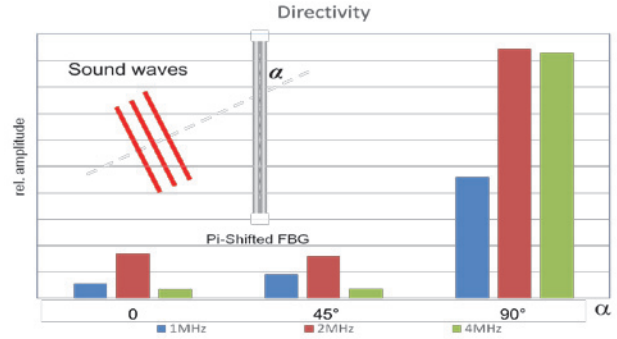

Fig. 8: Directivity of the π -shifted FBG sensors at 1 MHz, 2MHz and 4 MHz at 0°, 45°, and 90° incident angle of ultrasonic waves relative to the fiber sensor. At 90° incident angle the sensor sensitivities are higher than other cases.

Based on these results the π-shifted FBG sensors can be well applied in the frequency range till about 7 MHz, whereas the PVDF hydrophone shows constant sensitivity till 10 MHz. The strong sensing directivity of the π-shifted FBG sensors needs to be considered for applications.

Ultrasonic NDT Applications

For ultrasonic nondestructive testing (NDT) the π-shifted FBG sensors can be very interesting due to compact size, higher sensitivity at wide frequency range. In Fig. 9 a π-shifted FBG sensor was used for ultrasonic wave detection, where the fiber end was contacted with a glass block and coupled to it with a gel droplet. A small steel ball (diameter: 2.48 mm) was left fall down from the height of 1 m. The impulse energy could be used for ultrasonic wave excitation. On the glass cube a piezo transducer was applied for signal triggering (Fig. 9 upper). The signal showed a weak leading peak which was the longitudinal wave at higher sound speed. The Rayleigh waves with higher displacement amplitude at lower sound speed followed the longitudinal wave. This measurement results agreed with similar results in the literature [18].

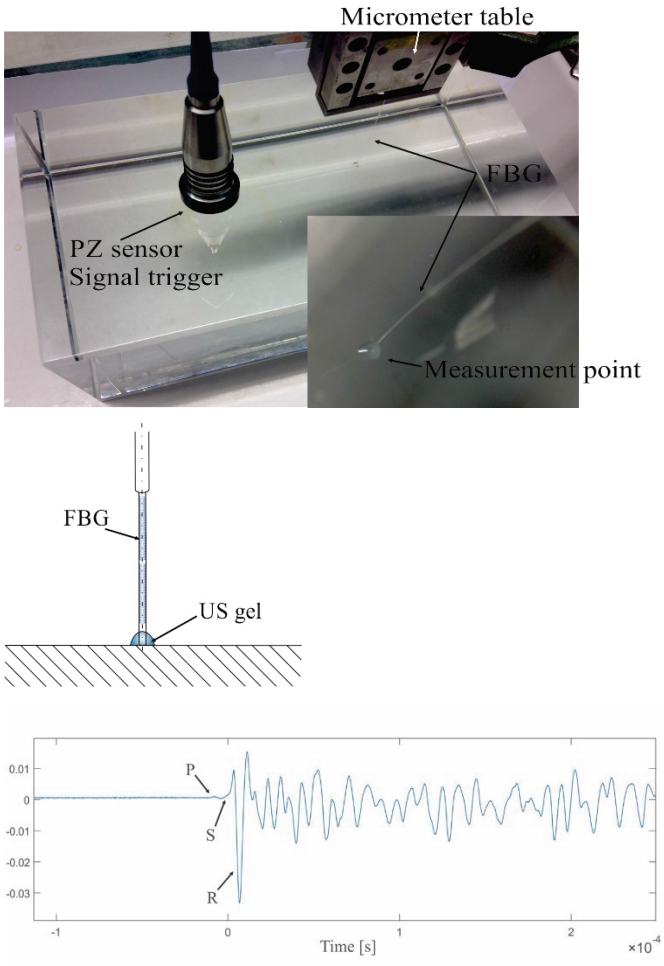

Fig. 9: Measurement result on a glass cube (upper), the fiber end of the π-shifted FBG sensor was contacted to the glass cube surface by using a gel droplet (middle), and the measurement signal shows the leading P-waves. After the Rayleigh waves (R-waves) fluctuations appear due to multi reflections of glass cube wall.

In many ultrasonic applications it is important to determine thicknesses of multiple layers or their sound velocities. A sample with a silicone layer (3.1 mm) on the acrylic glass sheet (0.8 mm) was investigated using the π-shifted FBG sensor (Fig. 10). An ultrasonic pulse echo system at 4 MHz was applied for the measurement. The sensing area of the π-shifted FBG sensor was located directly between the piezo transducer and silicone upper surface. A water droplet was used to couple the media (Fig. 10). Fig. 11 shows the measurement signals with the piezo transducer (blue) and with the π-shifted FBG sensor (red). Due to the narrow frequency band of the piezo transducer (less high frequency components) the echoes cannot be clearly separated. In case of the π-shifted FBG sensor the echoes from the interfaces silicone/acrylic glass and acrylic glass/air can be resolved due to the broad frequency response of the π-shifted FBG sensor.

Based on the time delay measurements (Δt = 6.55 µs) the sound velocities of the silicone layer can be estimated.

$$C_{silicone} = 947\ m/s$$

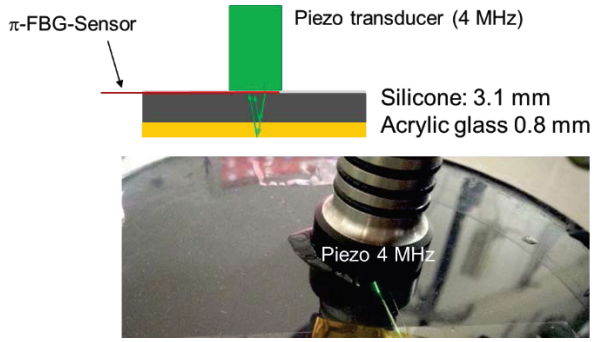

Fig. 10: The π-shifted FBG sensor was positioned between piezo transducer (4 MHz) and the silicone sample. In parallel an active π-shifted FBG sensor was used.

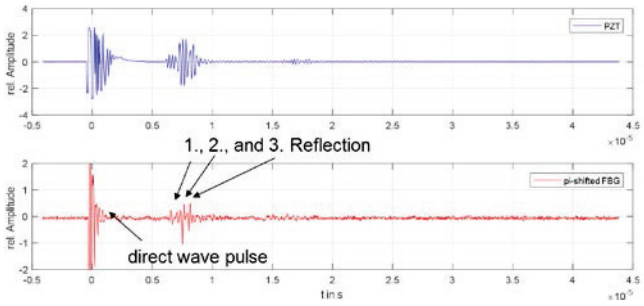

Fig. 11: Measurement signals with a piezo transducer at 4 MHz show the incident pulse and echoes (blue line), whereas the echoes can be resolved in the signals using the π-shifted FBG sensor (red line) due to the higher frequency bandwidth.

Conclusion

The primary investigations on the π-shifted FBG sensors show the applicability of this kind of optical sensors for nondestructive material testing or for medical applications. The π−shifted FBG sensors show the frequency response up to 7 MHz. At higher frequency (>7 MHz) the signal to noise ratio need to be considered. The incident angle of the sound waves to sensing area of the π−shifted FBG sensor has strong impact on the signal strength. The optimal incident angle is 90°. The reflected FBG spectrum can be simulated based on the transfer matrix method. In the future π-shifted FBG sensors will be further improved in terms of sensing characteristic for applications.

Literature

[1] Hocker G. B., “Fiber-optic sensing of pressure and temperature,” Applied Optics, vol. 18, pp. 1445–1448, 1979.

[2] Roriz, O. Frazão, A. B. Lobo-Ribeiro, J. L. Santos, and J. A. Simões, "Review of fiber-optic pressure sensors for biomedical and biomechanical applications," Journal of biomedical optics, vol. 18, p. 050903, 2013.

[3] Rao Y.-J., "Recent progress in applications of in-fibre Bragg grating sensors," Optics and lasers in Engineering, vol. 31, pp. 297-324, 1999.

[4] Kou J.-L., Ding M., Feng J., Lu Y.-Q., Xu F., and Brambilla G., "Microfiber-based Bragg gratings for sensing applications: a review," Sensors, vol. 12, pp. 8861-8876, 2012.

[5] Majumder M., Gangopadhyay T. K., Chakraborty A. K., Dasgupta K., and Bhattacharya D. K., "Fibre Bragg gratings in structural health monitoring—Present status and applications," Sensors and Actuators A: Physical, vol. 147, pp. 150-164, 2008.

[6] A. D. Kersey, "A review of recent developments in fiber optic sensor technology," Optical fiber technology, vol. 2, pp. 291-317, 1996.

[7] Kersey A., Davis M., Patrick H., LeBlanc M., Koo K., Askins C., Putnam M., and Friebele E., “Fiber grating sensors,” Journal of Lightwave Technology, vol. 15, no. 8, pp. 1442–1463, 1997. 1.1

[8] Rao Y., Webb D., Jackson D., Zhang L., and Bennion I., “High-resolution, wavelength-division-multiplexed in-fibre bragg grating sensor system,” Electronics Letters, vol. 32, no. 10, pp. 924–926, 1996. 1.1

[9] Fisher N., Webb D., Pannell C., Jackson D., Gavrilov L., Hand J., Zhang L., and Bennion I., “Ultrasonic hydrophone based on short in-fiber bragg gratings”, Applied optics, vol. 37, no. 34, pp. 8120–8128, 1998. 1.1

[10] Fomitchov P., Murray T., and Krishnaswamy S., “Intrinsic fiber-optic ultrasonic sensor array using multiplexed two-wave mixing interferometry,” Applied optics, vol. 41, no. 7, pp. 1262–1266, 2002.

[11] Fomitchov P. and Krishnaswamy S., “Response of a fiber bragg grating ultrasonic sensor,” Optical Engineering, vol. 42, pp. 956–963, 2003. 1.1, 4.3

[12] Wild G. and Hinckley S., "Acousto-ultrasonic optical fiber sensors: overview and state-of-the-art," IEEE Sensors journal, vol. 8, pp. 1184-1193, 2008

[13] Rosenthal A., Razansky D., and Ntziachristos V., “High-sensitivity compact ultrasonic detector based on a pi-phase-shifted fiber bragg grating,” Optics Letters, vol. 36, pp. 1833–1835, 2011. 1.1

[14] Wissmeyer G., Shnaiderman R., Soliman D., and Ntziachristos V., "Optoacoustic microscopy based on pi-FBG ultrasound sensors," in Photons Plus Ultrasound: Imaging and Sensing 2017, 2017, p. 1006423.

[15] Wissmeyer G., Soliman D., Shnaiderman R., Rosenthal A., and Ntziachristos V., "All-optical optoacoustic microscope based on wideband pulse interferometry," Optics letters, vol. 41, pp. 1953-1956, 2016.

[16] Hill K. O., Malo B., Bilodeau F., Johnson D., and Albert J., "Bragg gratings fabricated in monomode photosensitive optical fiber by UV exposure through a phase mask," Applied Physics Letters, vol. 62, pp. 1035-1037, 1993.

[17] Erdogan T., “Fiber grating spectra,” Journal of Lightwave Technology, vol. 15, pp. 1277–1294, 1997.

[18] Scruby C. B., Drain L. E., Laser Ultrasonics Techniques and Applications Adam Hilger 1990